Theoretical analysis of alendronate and risedronate effects on canine vertebral remodeling and microdamage

Xiang Wang [a], Antonia M. Erickson [a], Matthew R. Allen [b], David B. Burr [b,c], R. Bruce Martin [a], Scott J. Hazelwood [d,*]

[a] Lawrence J. Ellison Musculoskeletal Research Center, University of California Davis Medical Center, Sacramento, CA 95817, United States
[b] Department of Anatomy and Cell Biology, Indiana University School of Medicine, Indianapolis, IN 46202, United States
[c] Department of Orthopaedic Surgery, Indiana University School of Medicine, Indianapolis, IN 46202, United States
[d] Biomedical and General Engineering Department, California Polytechnic State University, San Luis Obispo, CA 93407, United States

A B S T R A C T

Bisphosphonates suppress bone remodeling activity, increase bone volume, and significantly reduce fracture risk in individuals with osteoporosis and other metabolic bone diseases. The objectives of the current study were to develop a mathematical model that simulates control and 1 year experimental results following bisphosphonate treatment (alendronate or risedronate) in the canine fourth lumbar vertebral body, validate the model by comparing simulation predictions to 3 year experimental results, and then use the model to predict potential long term effects of bisphosphonates on remodeling and microdamage accumulation. To investigate the effects of bisphosphonates on bone volume and microdamage, a mechanistic biological model was modified from previous versions to simulate remodeling in a representative volume of vertebral trabecular bone in dogs treated with various doses of alendronate or risedronate, including doses equivalent to those used for treatment of post-menopausal osteoporosis in humans. Bisphosphonates were assumed to affect remodeling by suppressing basic multicellular unit activation and reducing resorption area. Model simulation results for trabecular bone volume fraction, microdamage, and activation frequency following 1 year of bisphosphonate treatment are consistent with experimental measurements. The model predicts that trabecular bone volume initially increases rapidly with 1 year of bisphosphonate treatment, and continues to slowly rise between 1 and 3 years of treatment. The model also predicts that microdamage initially increases rapidly, 0.5–1.5-fold for alendronate or risedronate during the first year of treatment, and reaches its maximum value by 2.5 years before trending downward for all dosages. The model developed in this study suggests that increasing bone volume fraction with long term bisphosphonate treatment may sufficiently reduce strain and damage formation rate so that microdamage does not accumulate above that which is initiated in the first two years of treatment.

1. Introduction

Bisphosphonates (BPs) are anti-resorptive drugs that suppress bone remodeling, increase bone volume and bone mineral density, and are used to treat post-menopausal osteoporosis and other bone fragility disorders (Rodan and Fleisch, 1996; Chavassieux et al., 1997; Tonino et al., 2000; Ding et al., 2003; Dufresne et al., 2003; Recker et al., 2005). At the tissue level in humans, BP treatment is associated with decreased bone resorption and turnover (Storm et al., 1993; Rodan and Fleisch, 1996; Eriksen et al., 2002) and, therefore, provides a transient increase in bone volume (filling of pre-existing remodeling spaces). This may be followed by a further trend to increase bone volume by reducing the amount of bone resorbed relative to that formed by basic multicellular units (BMUs) (Boyce et al., 1995). In post-menopausal women, BPs reduce fracture risk by improving the structural properties of bone (Delmas, 2000) and increasing the degree of mineralization (Boivin et al., 2000). However, BP treatment also results in significant microdamage accumulation and a reduction in bone toughness in canine vertebrae (Mashiba et al., 2001; Komatsubara et al., 2003; Allen et al., 2006; Allen and Burr, 2007). The microdamage accumulation is due, at least in part, to decreased remodeling, which is the only mechanism in bone to remove fatigue damage (Burr et al., 1985; Mori and Burr, 1993). These observations, some having positive and others negative implications in bone, indicate the need for a better understanding of BP effects on bone remodeling, structure, and material properties.

While long term BP studies have focused on alterations to bone mineral density and bone turnover (Miller et al., 1997; Tonino et al., 2000; Bone et al., 2004; Ste-Marie et al., 2004; Borah et al., 2006; Zoehrer et al., 2006), their effects on microdamage accumulation have not been studied beyond 3 years of treatment (Forwood et al., 1995; Hirano et al., 2000; Mashiba et al., 2000, 2005, 2001; Komatsubara et al., 2003, 2004; Day et al., 2004; Allen et al., 2006, Allen and Burr, 2007). Results from canine studies have documented microdamage increases in the vertebral body, rib, and ilium following 1–3 years of BP treatment, but these changes were compensated for by increases in bone mass and structural properties, including ultimate load and stiffness (Allen and Burr, 2007). However, some of these studies also documented significant reductions in bone toughness, the intrinsic ability of the tissue to resist fracture. Since BP treatment in patients with osteoporosis now extends 10 years or more, the long term effects of BPs on microdamage accumulation and bone fragility are of clinical interest.

In the present study, we develop a mathematical model to explore the long term effects of BP treatment on bone. We have previously developed computational models simulating bone mechanics and remodeling in a representative volume of bone (Martin, 1995; Hazelwood et al., 2001; Nyman et al., 2004, 2006). These models simulate BMU activation and remodeling in response to mechanical loading and fatigue microdamage. Our overall goal in developing these mathematical models is to simulate the long term effects of BPs on remodeling and microdamage accumulation in current animal models and, ultimately, in humans. As an initial step, our approach in the current study is to develop a model of remodeling in a representative volume of trabecular bone based on control and 1 year experimental results following BP treatment in the canine fourth lumbar vertebral body (Allen et al., 2006), and subsequently to test its predictions against data from a 3 year alendronate study (Allen and Burr, 2007). Then, in an effort to understand long term bisphosphonate treatment effects over periods similar to those for clinical use in humans, we examine model predictions after 10 years of simulated treatment.

2. Methods

The control and 1 year data used for model development were from skeletally mature female beagles treated daily with saline vehicle or one of three doses of alendronate (ALN: 0.10, 0.20, or 1.00 mg/kg/day) or risedronate (RIS: 0.05, 0.10, or 0.50 mg/kg/day) (Allen et al., 2006). The middle doses of ALN and RIS correspond to the clinical treatment dose, on a mg/kg basis, for post-menopausal osteoporosis. The lower dose of ALN corresponds to the preventative dose for osteoporosis, while the higher dose of both ALN and RIS are approximately equivalent to those used for treatment of Paget's disease. In that study, trabecular bone mineral density (BMD, g/cm^3), volume fraction (BV/TV), activation frequency (Ac.f), and microdamage (crack surface density or Cr.S.Dn) in the fourth lumbar vertebra (L4) were quantified.

A previous bone remodeling algorithm (Hazelwood et al., 2001; Nyman et al., 2004) was modified to simulate remodeling in a 1 cm^3 volume of canine L4 vertebral trabecular bone under uniaxial cyclic loading. The model describes histomorphometric variables governing bone mechanical properties (Table 1). The cancellous bone structure was assumed to be isotropic with a uniform bone volume fraction, BV/TV. The continuum-level elastic modulus (E) was assumed to be related to BV/TV by

$$E = E_0(\mathrm{BV/TV})^b, \tag{1}$$

where $E_0 = 19{,}735$ MPa and $b = 2.4217$ were obtained by fitting experimental data from control and 1 year BP-treated dogs to Eq. (1) (Table 2). Peak strain was calculated as

$$\varepsilon = \sigma/E, \tag{2}$$

where σ is the peak stress applied during cyclic loading.

A loading potential, Φ, was defined to characterize the mechanical environment as it affects remodeling (Hazelwood et al., 2001)

$$\Phi = R_L \varepsilon^q, \tag{3}$$

Table 1
Model state variables.

	State variable
E	Elastic modulus (MPa)
BV/TV	Bone volume fraction
N.Rs.BMU	Number of resorbing BMUs (# BMU/mm^2)
N.F.BMU	Number of refilling BMUs (# BMU/mm^2)
Ac.f	BMU activation frequency (# BMU/mm^2/day)
Ac.f$_{year}$	BMU activation frequency (# BMU/year)
BS/TA	Bone surface area per section area
Cr.S.Dn	Microdamage (mm/mm^2)
σ	Peak stress of cyclic compressive loading
ε	Peak strain of cyclic compressive loading
Φ	Mechanical stimulus (cycles per day, cpd)

where R_L is the loading frequency (assumed to be constant at 3000 cycles per day), and $q = 4$ adjusts the relative contribution of peak strain and loading frequency to the loading potential.

2.1. Microdamage

Microdamage (Cr.S.Dn) was defined as cumulative microcrack length per unit cross-sectional area of bone (mm/mm^2). The damage formation rate was assumed to be proportional to the loading potential

$$\left(\frac{\mathrm{dCr.S.Dn}}{\mathrm{dt}}\right)_F = k_D \Phi, \tag{4}$$

where k_D is chosen to make the damage formation and removal rates equal under steady state conditions (Hazelwood et al., 2001).

The fatigue microdamage removal rate was modeled as (Martin, 1995)

$$\left(\frac{\mathrm{dCr.S.Dn}}{\mathrm{dt}}\right)_{Rs} = \mathrm{Cr.S.Dn} \cdot \mathrm{Ac.f} \cdot \mathrm{Rs.Ar} \cdot F_s, \tag{5}$$

where Ac.f is the BMU activation frequency, Rs.Ar is the resorption space area, and F_s is a "steering factor" to account for targeted damage removal (Martin, 1985). Hence, the net damage accumulation rate is

$$\frac{\mathrm{dCr.S.Dn}}{\mathrm{dt}} = \left(\frac{\mathrm{dCr.S.Dn}}{\mathrm{dt}}\right)_F - \left(\frac{\mathrm{dCr.S.Dn}}{\mathrm{dt}}\right)_{Rs}. \tag{6}$$

2.2. Bone volume fraction

The time rate of change of bone volume fraction, d(BV/TV)/dt, was assumed to be a function of the mean bone resorption (Rs.Ar/Rs.P) and refilling (FAr/FP) rates within individual BMUs, and the mean densities of resorbing (N.Rs.BMU) and refilling (N.F.BMU) BMUs (Martin, 1985)

$$\frac{\mathrm{d(BV/TV)}}{\mathrm{dt}} = \frac{\mathrm{FAr}}{\mathrm{FP}}\,\mathrm{N.F.BMU} - \frac{\mathrm{Rs.Ar}}{\mathrm{Rs.P}}\,\mathrm{N.Rs.BMU}, \tag{7}$$

$$\mathrm{N.F.BMU} = \int_{t-(\mathrm{Rs.P+Rv.P+FP})}^{t-(\mathrm{Rs.P+Rv.P})} \mathrm{Ac.f}\,\mathrm{dt}', \tag{8}$$

$$\mathrm{N.Rs.BMU} = \int_{t-\mathrm{Rs.P}}^{t} \mathrm{Ac.f}\,\mathrm{dt}', \tag{9}$$

where Rs.Ar and FAr are the mean resorption and refilling areas and Rs.P and FP are the mean resorption and refilling periods, respectively, of individual BMUs (Table 2). The shape of the BMU resorption cavity was modeled as a semi-ellipse having a mean cross-sectional area of 0.014 mm^2 as measured from the control dogs (previously unpublished data (Allen et al., 2006)).

2.3. BMU activation frequency

BMU Ac.f (BMUs/mm^2/day) was assumed to be a function of disuse, microdamage, and the available surface area for remodeling, BS/TA. This leads to the equation

$$\mathrm{Ac.f} = (\mathrm{Ac.f_{damage}} + \mathrm{Ac.f_{disuse}})\frac{\mathrm{BS/TA}}{(\mathrm{BS/TA})_{max}}, \tag{10}$$

Table 2
Model constants.

	Constant	Values	Source
E_0	Tissue modulus (MPa)	19735	Calculated[a]
b	Modulus-BV/TV exponent	2.4217	Calculated[a]
Rs.Ar	Resorption area, mm^2	0.01395	Measured[a]
FAr	Refilling area, mm^2	0.01395	Assumed equal to Rs.Ar
C_F	Ratio of FAr to Rs.Ar$_{(BP)}$	1.45–2	–
Rs.Ar$_{(BP)}$	BP treatment resorption area, mm^2	FAr/C_F	–
E.De	Erosion cavity depth, mm	0.0667	Measured[a]
E.Wi	Erosion cavity width, mm	0.293	Measured[a]
Md.S.Le	Mean mineralized bone surface length, mm	0.1935	Measured[a]
Rs.P	Resorption period, days	10	Measured[a]
Rv.P	Reversal period, days	5	(Nyman et al., 2004)
FP	Refilling period, days	44	Measured[a]
k_D	Damage rate coefficient, mm/mm^2	11×10^5	Estimated[b]
q	Damage rate exponent	4	(Whalen et al., 1988; Hazelwood et al., 2001)
R_L	Loading rate, cpd	3000	(Hazelwood et al., 2001)
F_s	Damage removal specificity factor	20	Estimated[b]
Cr.S.Dn$_0$	Threshold damage, mm/mm^2	0.01	Estimated[b]
Ac.f$_0$	Threshold BMU activation frequency, BMUs/mm^2/day	0.08	Estimated[b]
Φ_0	Threshold mechanical stimulus, cpd	1.875×10^{-10}	(Beaupre et al., 1990)
Ac.f$_{max}$	Maximum BMU activation frequency, BMUs/mm^2/day	0.50	(Frost, 1969; Schaffler et al., 1995)
k_b	activation frequency dose-response coefficient, cpd^{-1}	6.5×10^{10}	(Hazelwood et al., 2001)
k_c	activation frequency dose-response coefficient, cpd	9.4×10^{-11}	(Hazelwood et al., 2001)
k_r	activation frequency coefficient	−1.6	(Hazelwood et al., 2001)
P_{max}	Maximum potency	1	(Nyman et al., 2004)
τ_s	Coefficient	1–50	(Nyman et al., 2004)

[a] Previously unpublished data measured or calculated from the specimens of Allen et al. (2006).
[b] Parameters estimated in the model simulation to produce steady state values for Ac.f, Cr.S.Dn, and BV/TV similar to the remodeling data for controls and 1 year experiments.

$$\text{Ac.f}_{\text{damage}} = \begin{cases} \dfrac{\text{Ac.f}_0\,\text{Ac.f}_{\max}}{\text{Ac.f}_0 + (\text{Ac.f}_{\max} - \text{Ac.f}_0)\exp(k_r\,\text{Ac.f}_{\max}(\text{Cr.S.Dn} - \text{Cr.S.Dn}_0)/\text{Cr.S.Dn}_0)} & \text{Cr.S.Dn} > \text{Cr.S.Dn}_0 \\ \text{Ac.f}_0\,(\text{Cr.S.Dn}/\text{Cr.S.Dn}_0) & \text{Cr.S.Dn} \leqslant \text{Cr.S.Dn}_0 \end{cases}, \tag{11}$$

$$\text{Ac.f}_{\text{disuse}} = \begin{cases} \dfrac{\text{Ac.f}_{\max}}{1+\exp(k_b\,(\Phi - k_c))} & \Phi < \Phi_0 \\ 0 & \Phi \geqslant \Phi_0 \end{cases}, \tag{12}$$

where Ac.f$_{damage}$ and Ac.f$_{disuse}$ represent the BMU activation frequencies associated with microdamage and disuse, respectively, and are assumed to be independent remodeling responses. Specific surface area was determined from BV/TV using an empirical relationship,

$$\text{BS/TA} = 32.3(1-\text{BV/TV}) - 93.9(1-\text{BV/TV})^2 + 134(1-\text{BV/TV})^3 - 101(1-\text{BV/TV})^4 + 28.8(1-\text{BV/TV})^5 \tag{13}$$

normalized by the maximum value, $(\text{BS/TA})_{max} = 4.191\,\text{mm}^{-1}$ (Hazelwood et al., 2001).

To compare simulation predictions with experimental results, the annual activation frequency (Ac.f$_{year}$, BMU/year) was calculated as (Nyman et al., 2004)

$$\text{Ac.f}_{\text{year}} = 365\,\frac{\text{Md.S.Le}\cdot\text{Ac.f}}{\text{BS/TA}}, \tag{14}$$

where Md.S.Le is the mean mineralized length of a BMU's active surface (Table 2).

2.4. Bisphosphonate effects

Bisphosphonate treatment was assumed to (1) suppress BMU activation frequency (Storm et al., 1993; Chavassieux et al., 1997, 2000; Eriksen et al., 2002) and (2) reduce resorption cavity depth (Boyce et al., 1995). A potency variable, P, was defined to quantify the BP's ability to suppress remodeling activation (Nyman et al., 2004)

$$P = P_{\max}(1 - \exp(-\tau_s\,\text{N.Rs.BMU})), \tag{15}$$

where N.Rs.BMU is the number of resorbing BMUs, $P_{max} = 1$ is the fully suppressed potency, and τ_s is a suppression coefficient (Table 3). The activation frequency was suppressed by multiplying Ac.f by $(1-P)$, where P has a value between 0 and 1. Resorption cavity area (Rs.Ar) was also assumed to be reduced, depending on the type and dosage of BP treatment (Nyman et al., 2004). A refilling coefficient describing the balance between bone formed and resorbed at each resorption site was defined as

$$C_F = \frac{\text{FAr}}{\text{Rs.Ar}_{(BP)}}, \tag{16}$$

where Rs.Ar$_{(BP)}$ is the reduced resorption cavity area dependent on the BP administered and dosage (Table 2).

2.5. Numerical simulation

All simulations were performed in MATLAB (MathWorks, Natick, MA). The model was implemented using a time step of 1 day. An equilibrium status of trabecular bone remodeling that matched the experimental control data for canine vertebral trabecular bone was obtained first (Table 4). For a BV/TV of 22.3% (Allen et al., 2006) in a 1 cm^3 representative volume of trabecular bone, it was found that a peak cyclic stress of $\sigma = 0.265$ MPa produces steady state values for the principal outcome variables Ac.f, Cr.S.Dn, and BV/TV similar to the remodeling data of the control dogs. Then, using the equilibrium condition as the baseline, the model was used to find values of the bisphosphonate variables τ_s and C_F that matched the 1 year canine experimental data (Tables 3 and 4). Because BPs suppress bone turnover soon after treatment initiation (Porras et al., 1999), their effects were assumed to begin immediately.

The simulation then was carried out for 3 years of BP treatment and results were compared to recent 3 year experimental data available for the fourth lumbar vertebral body in canines at the middle (0.20 mg/kg/day) and high (1.00 mg/kg/day) doses of alendronate treatment (Allen and Burr, 2007). Finally, the model was used to predict the effects on remodeling and damage accumulation after 10 years of BP treatment to provide an understanding of longer term bisphosphonate use at periods similar to those for human osteoporosis patients.

Comparisons of simulation predictions to experimental results were made by examining the similarity of the values in comparison to the measured standard deviation and by a one sample t-test ($p<0.05$ significant) with the hypothesis that the simulation values represent the experimental means.

Table 3
Sensitivity analysis of bisphosphonate effects simulated by the model.

Bisphosphonate	Dosage (mg/kg/day)	Suppression coefficient τ_s	Refilling coefficient C_F
ALN	0.10	11.3	1.70
	0.20	18.8	1.80
	1.00	38	2.00
RIS	0.05	5	1.45
	0.10	11	1.65
	0.50	50	2.00

Table 4
Model predictions and experimental measurements in the canine vertebral body after 1 year of ALN or RIS treatment.

Treatment	Variable	Simulation	Experiment
Control	BV/TV	0.223	0.219 ± 0.031
	Cr.S.Dn (mm/mm^2)	0.0135	0.0068 ± 0.0073
	Ac.f$_{year}$ (# BMUs/year)	1.70	1.89 ± 0.84
1 year ALN 0.10 mg/kg/day	BV/TV	0.252	0.257 ± 0.052
	Cr.S.Dn	0.0198	0.0210 ± 0.0178
	Ac.f$_{year}$	0.64	0.66 ± 0.38
1 year ALN 0.20 mg/kg/day	BV/TV	0.252	0.264 ± 0.036
	Cr.S.Dn	0.0252	0.0250 ± 0.0140
	Ac.f$_{year}$	0.45	0.54 ± 0.24
1 year ALN 1.00 mg/kg/day	BV/TV	0.252	0.259 ± 0.044
	Cr.S.Dn	0.0321	0.0322 ± 0.0212
	Ac.f$_{year}$	0.26	0.45 ± 0.27
1 year RIS 0.05 mg/kg/day	BV/TV	0.244	0.254 ± 0.038
	Cr.S.Dn	0.0140	0.0199 ± 0.0075
	Ac.f$_{year}$	1.04	1.13 ± 0.65
1 year RIS 0.10 mg/kg/day	BV/TV	0.250	0.231 ± 0.038
	Cr.S.Dn	0.0197	0.0200 ± 0.0121
	Ac.f$_{year}$	0.65	0.65 ± 0.38
1 year RIS 0.50 mg/kg/day	BV/TV	0.251	0.263 ± 0.037
	Cr.S.Dn	0.0344	0.0370 ± 0.0195
	Ac.f$_{year}$	0.21	0.31 ± 0.31

3. Results

As expected, the simulated results following 1 year of BP treatment are consistent with experimental measurements (Table 4). At 1 year, the model predicts that the high dose of ALN will suppress Ac.f by 85% compared to 62% for the low dose. The equivalent values predicted for RIS are much more widely spread at 87% and 39%, respectively (Fig. 1). At the doses used for treatment of human post-menopausal osteoporosis, ALN (0.20 mg/kg/day) and RIS (0.10 mg/kg/day) reduce the number of active BMUs per year to 0.45 and 0.65, respectively. The model predicts that 1 year of ALN treatment increases BV/TV approximately 13% (Fig. 2) compared to 9.7–13% for RIS depending on dose (Fig. 3). Microdamage is predicted to reach its maximum within the first year for the low dose of ALN (Fig. 2) or RIS (Fig. 3) treatment. For the middle and high doses of ALN and RIS, Cr.S.Dn is predicted to increase rapidly by 46% to 155% after 1 year of treatment. All predicted Ac.f, BV/TV, and Cr.S.Dn values at 1 year of treatment are within one standard deviation of their corresponding experimental measurements. The *t*-test analysis indicates a similarity between experimental results and their corresponding model predictions for all values at 1 year of BP treatment except for Ac.f for ALN at the high dose ($p = 0.03$) and Cr.S.Dn for RIS at the low dose ($p = 0.02$).

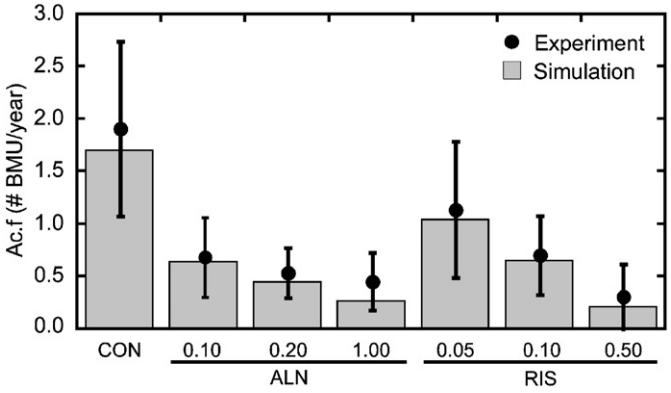

Fig. 1. Ac.f$_{year}$ decreases in relation to control after 1 year of ALN and RIS treatment. The error bars represent one standard deviation. CON represents the control data. ALN 0.10 refers to an alendronate dose of 0.10 mg/kg/day, etc.

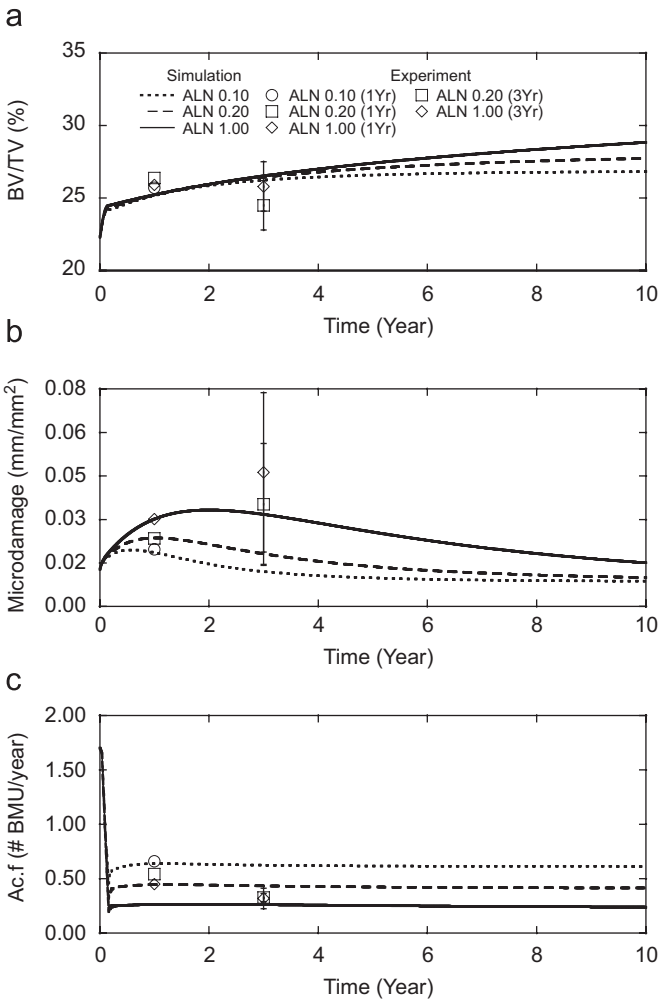

Fig. 2. Predictions for BV/TV, Cr.S.Dn and Ac.f during 3 years of ALN treatment. Time = 0 represents the beginning of ALN treatment. ALN 0.10 refers to an alendronate dose of 0.10 mg/kg/day, etc. The error bars represent ±1 standard deviation.

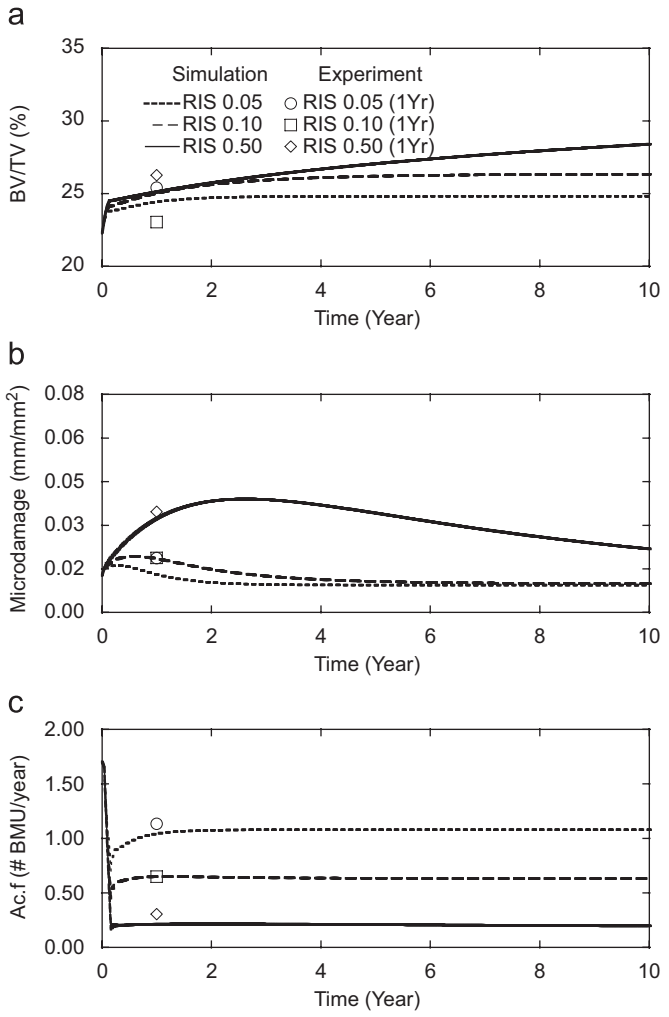

Fig. 3. Predictions for BV/TV, Cr.S.Dn and Ac.f during 3 years of RIS treatment. Time = 0 represents the beginning of RIS treatment. RIS 0.05 refers to a risedronate dose of 0.05 mg/kg/day, etc.

The model predicts modest additional increases in bone volume fraction between 1 and 3 years of treatment (Table 5). For ALN, the percent increase in BV/TV from the 1 year predictions ranges from 4.2% at the low dose to 5.2% at the high dose (Fig. 2). For RIS, the increase in BV/TV ranges from 1.5% to 4.5% between the low and high doses, respectively (Fig. 3). In addition, the simulation predicts slight changes in Ac.f for ALN (−0.72% to −2.6%) and RIS (−1.5% to 3.4%) between 1 and 3 years of treatment.

Due to the bisphosphonate-induced inhibition of remodeling, resulting in a greater initial decline in the damage removal rate than the damage formation rate (Fig. 4), microdamage is predicted to increase during the first year of treatment. Within 3 years, Cr.S.Dn reaches its maximum value and thereafter trends downward at greatly varying rates depending on the dosage of ALN or RIS (Figs. 2 and 3). Compared to 1 year of treatment, the model predicts a 26% decrease in Cr.S.Dn after 3 years of low dose (0.05 mg/kg/day) RIS treatment. Under the high dose RIS regimen, Cr.S.Dn continues to increase throughout the second year and

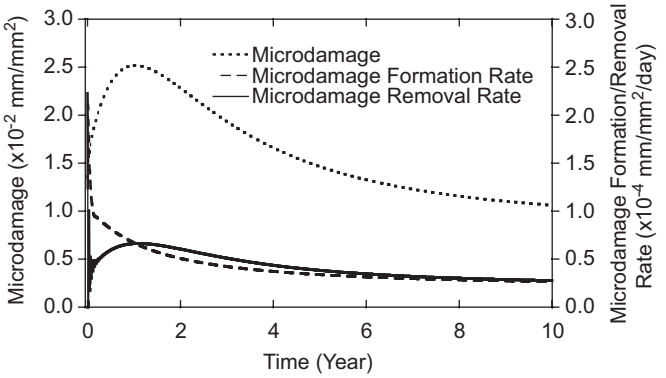

Fig. 4. In the dogs subjected to the middle dose of ALN (0.20 mg/kg/day), the simulation predicts that microdamage formation and removal rates initially decrease sharply after BP administration. As the microdamage formation rate continues to decline over time due to further increases in BV/TV, the damage removal rate recovers as a result of increases in Ac.f. As the microdamage removal rate surpasses the formation rate, damage accumulation declines. Similar patterns were observed for all doses of ALN and RIS.

Table 5
Model predictions for changes in the canine vertebral body after 3 years of ALN or RIS treatment.

Treatment	Variable	Simulation	Change from 1 year simulation result (%)	Experiment[a]
3 year ALN 0.10 mg/kg/day	BV/TV	0.262	4.21	–
	Cr.S.Dn (mm/mm^2)	0.0128	−35.35	–
	Ac.f$_{year}$ (# BMU/year)	0.62	−2.25	–
3 year ALN 0.20 mg/kg/day	BV/TV	0.264	4.84	0.245 ± 0.017
	Cr.S.Dn	0.0193	−23.41	0.0376 ± 0.0223
	Ac.f$_{year}$	0.43	−2.58	0.328 ± 0.037
3 year ALN 1.00 mg/kg/day	BV/TV	0.265	5.15	0.258 ± 0.017
	Cr.S.Dn	0.0338	5.30	0.0493 ± 0.0293
	Ac.f$_{year}$	0.26	−0.72	0.319 ± 0.094
3 year RIS 0.05 mg/kg/day	BV/TV	0.248	1.47	–
	Cr.S.Dn	0.0103	−26.42	–
	Ac.f$_{year}$	1.08	3.43	–
3 year RIS 0.10 mg/kg/day	BV/TV	0.259	3.59	–
	Cr.S.Dn	0.0133	−32.49	–
	Ac.f$_{year}$	0.64	−1.49	–
3 year RIS 0.50 mg/kg/day	BV/TV	0.262	4.50	–
	Cr.S.Dn	0.0414	20.35	–
	Ac.f$_{year}$	0.21	0.70	–

[a] Three year experimental data are available for only the 0.20 mg/kg/day and 1.00 mg/kg/day ALN treatments (Allen and Burr, 2007).

starts to diminish in the third year of treatment, reaching a damage burden at 3 years that is 20% above that at 1 year. The dynamics are similar for ALN, and for both bisphosphonates the maximum amounts of Cr.S.Dn predicted at 3 years increase with increasing dosage. For both ALN and RIS, the lowest dose allows a faster return to a low damage burden compared to the higher doses.

Predicted BV/TV, Cr.S.Dn, and Ac.f results at 3 years of treatment are at or within one standard deviation of the corresponding experimental measurements in all cases except for Ac.f at the middle dose of ALN which is 2.8 standard deviations different. The statistical analysis indicates significant differences for experimental results compared to predicted values for the middle dose ($0 < p < 0.02$) but similarities for all values at the high dose after 3 years of treatment.

Depending on dose, the model predicts long term bisphosphonate treatment for 10 years to produce BV/TV increases of 20–29% for ALN (Fig. 2a) and 11–27% for RIS (Fig. 3a) compared to controls. Running the present model out to 10 years of treatment produces steady state values of Ac.f after approximately 2.5 years for RIS (Fig. 3c) and 3.5 years for ALN (Fig. 2c) that are 64–86% below the untreated controls for ALN and 36–88% below controls for RIS depending on dose. Microdamage accumulation (Figs. 2b and 3b) is also dose-dependent and reaches its peak between 0.3 and 2.5 years (more quickly for lower doses). Microdamage reaches a steady state value (0.0093 mm/mm^2) slightly below the untreated controls after 8 years of ALN treatment for the low dose. After 10 years of the high dose RIS treatment, Cr.S.Dn (0.0233 mm/mm^2) is greater than those of the middle (0.0105 mm/mm^2) and low (0.0100 mm/mm^2) dose treatments. With the middle and high doses of ALN or the high dose of RIS, Cr.S.Dn continues to decline even after 10 years of treatment.

4. Discussion

Bisphosphonates are widely used to treat human post-menopausal osteoporosis and have well-established anti-fracture efficacy. Experiments on canines involving 1 year of bisphosphonate treatment at various doses (including those used to treat post-menopausal osteoporosis) show suppressed bone remodeling activity; increased bone volume fraction, mineralization, stiffness, and microdamage accumulation; and reduced bone toughness (Mashiba et al., 2001; Komatsubara et al., 2003; Allen et al., 2006). The goal of the current study was to develop a computational model to simulate the effects of BPs on bone remodeling based on 1 year experimental data from canine vertebrae and then examine results simulating long term BP use.

For varying doses of ALN or RIS, our model predicts a sharp decline in activation frequency during the first two months of treatment. Subsequently, Ac.f increases slightly, reaching a new equilibrium after 2–5 years of treatment. The degree of Ac.f decline is consistent with 1 year experimental data (Allen et al., 2006), and its predicted long term steady state results are dose-dependent, with the three doses of RIS having a wider variation in long term results compared to the ALN doses.

In the simulation, microdamage accumulates rapidly within the first 3 years of BP treatment. Although the microdamage formation rate initially decreases sharply as a result of increases in BV/TV, which reduces the strain level in the representative bone volume, the initial decrease in the damage removal rate due to the Ac.f reduction is greater (Fig. 4). Then Ac.f and, subsequently, the damage removal rate begin to recover. Eventually, within 0.3–2.5 years depending on dose, the damage removal rate surpasses the diminished damage formation rate, and the burden of damage due to remodeling inhibition declines. These data predict that microdamage accumulation will be of greatest concern in the short-term following the initiation of BP treatment, prior to the point where bone volume increases sufficiently to reduce local strain. This is consistent with data from the 1 and 3 year experiments that show a significant increase in damage at 1 year but no difference between 1 and 3 years of ALN treatment (Allen and Burr, 2007). These results suggest that the reduced level of remodeling may be sufficient to control microdamage accumulation during long term BP treatment. The model predicts that ultimately, after 8 years of ALN treatment for the low dose, a new equilibrium is reached with a damage burden about 31% lower than that of the untreated baseline controls. For RIS the return to a steady state requires approximately 3–8 years for the low and middle doses, with damage at 10 years predicted to be 26% less for the low dose and 22% less for the middle dose relative to baseline controls.

One of the strengths of the current study is the ability to compare the simulation results with those from a well-designed experiment with control animals to represent the equilibrium status before BP treatment. Data on the effects of BP treatment on BV/TV, Ac.f, and Cr.S.Dn provide a foundation for defining the "dose-response coefficients" for the effects of the bisphosphonates examined. That the present model reasonably predicts the 3 year experimental work demonstrates the appropriateness of the coefficients chosen for the simulation and forms a basis to explore BP effects over time periods consistent with post-menopausal life spans.

However, the present work clearly has significant limitations. The bone remodeling process is simplified in the model. For example, variability in the size and shape of resorption cavities, and many other aspects of the remodeling process, are not represented in the present computer simulation. Furthermore, the present model only simulates bone volume fraction as governed by remodeling within trabecular bone, and does not consider the microarchitecture of trabecular bone or the effects of cortical bone. Neither does it consider bone modeling activities that may affect bone fragility (Frost, 1998). The effects of remodeling are only considered with regard to elastic modulus; certainly bisphosphonates are expected to affect strength and toughness as well.

Experimental results show increased trabecular bone stiffness after BP treatment, but no difference in elastic modulus, ultimate load, or ultimate stress (Allen et al., 2006). However, our simulation results indicate 1 year of BP treatment increases not only BV/TV but also elastic modulus in ALN- and RIS-treated animals compared to controls. One explanation for this discrepancy is that the effects of BP treatment on the degree of bone mineralization (Allen et al., 2006), which significantly affects elastic modulus and other mechanical properties (Moore and Gibson, 2002; Wang and Niebur, 2006), was not considered in the model.

Over time, many of these limitations may be overcome by developing more detailed models in conjunction with ongoing experimental work and the accumulation of human data. In the meantime, the present simulation and experimental results suggest that the effects of bisphosphonates on bone remodeling may not lead to bone fragility associated with microdamage accumulation, and are consistent in that regard with 10 year alendronate treatment data for humans (Bone et al., 2004). Further work is needed, however, before this and other clinical questions can be answered.

Conflict of interest statement

MRA and DBB have received financial support from Eli Lilly, The Alliance for Better Bone Health (Procter and Gamble), and Amgen. In addition, DBB serves as an advisor for Eli Lilly and

Merck, and as a speaker for Eli Lilly, The Alliance for Better Bone Health, Amgen, Roche, and GlaxoSmithKline. XW, AME, RBM, and SJH disclose that they do not have conflicts of interest regarding the work presented in this manuscript.

Acknowledgements

This work was supported by NIH Grants R01 AR51555, R01 AR047838, and T32 AR007581, and a research grant from The Alliance for Better Bone Health (Procter and Gamble Pharmaceuticals and Sanofi-Aventis). Merck and Co. kindly provided the alendronate. This investigation utilized an animal facility constructed with support from Research Facilities Improvement Program Grant no. C06RR10601 from the NIH National Center for Research Resources.

References

Allen, M.R., Burr, D.B., 2007. Three years of alendronate treatment results in similar levels of vertebral microdamage as after one year of treatment. Journal of Bone and Mineral Research 22 (11), 1759–1765.

Allen, M.R., Iwata, K., Phipps, R., Burr, D.B., 2006. Alterations in canine vertebral bone turnover, microdamage accumulation, and biomechanical properties following 1-year treatment with clinical treatment doses of risedronate and alendronate. Bone 39 (4), 872–879.

Beaupre, G.S., Orr, T.E., Carter, D.R., 1990. An approach for time-dependent bone modeling and remodeling-application: a preliminary remodeling simulation. Journal of Orthopaedic Research 8 (5), 662–670.

Boivin, G.Y., Chavassieux, P.M., Santora, A.C., Yates, J., Meunier, P.J., 2000. Alendronate increases bone strength by increasing the mean degree of mineralization of bone tissue in osteoporotic women. Bone 27 (5), 687–694.

Bone, H.G., Hosking, D., Devogelaer, J.P., Tucci, J.R., Emkey, R.D., Tonino, R.P., Rodriguez-Portales, J.A., Downs, R.W., Gupta, J., Santora, A.C., Liberman, U.A., Alendronate Phase III Osteoporosis Treatment Study Group, 2004. Ten years' experience with alendronate for osteoporosis in postmenopausal women. New England Journal of Medicine 350 (12), 1189–1199.

Borah, B., Dufresne, T.E., Ritman, E.L., Jorgensen, S.M., Liu, S., Chmielewski, P.A., Phipps, R.J., Zhou, X., Sibonga, J.D., Turner, R.T., 2006. Long-term risedronate treatment normalizes mineralization and continues to preserve trabecular architecture: sequential triple biopsy studies with micro-computed tomography. Bone 39 (2), 345–352.

Boyce, R.W., Paddock, C.L., Gleason, J.R., Sletsema, W.K., Eriksen, E.F., 1995. The effects of risedronate on canine cancellous bone remodeling: three-dimensional kinetic reconstruction of the remodeling site. Journal of Bone and Mineral Research 10 (2), 211–221.

Burr, D.B., Martin, R.B., Schaffler, M.B., Radin, E.L., 1985. Bone remodeling in response to in vivo fatigue microdamage. Journal of Biomechanics 18, 189–200.

Chavassieux, P.M., Arlot, M.E., Reda, C., Wei, L., Yates, A.J., Meunier, P.J., 1997. Histomorphometric assessment of the long-term effects of alendronate on bone quality and remodeling in patients with osteoporosis. Journal of Clinical Investigation 100, 1475–1480.

Chavassieux, P.M., Arlot, M.E., Roux, J.P., Portero, N., Daifotis, A., Yates, A.J., Hamdy, N.A., Malice, M.P., Freedholm, D., Meunier, P.J., 2000. Effects of alendronate on bone quality and remodeling in glucocorticoid-induced osteoporosis: a histomorphometric analysis of transiliac biopsies. Journal of Bone and Mineral Research 15, 754–762.

Day, J.S., Ding, M., Bednarz, P., van der Linden, J.C., Mashiba, T., Hirano, T., Johnston, C.C., Burr, D.B., Hvid, I., Sumner, D.R., Weinans, H., 2004. Bisphosphonate treatment affects trabecular bone apparent modulus through micro-architecture rather than matrix properties. Journal of Orthopaedic Research 22 (3), 465–471.

Delmas, P.D., 2000. How does antiresorptive therapy decrease the risk of fracture in women with osteoporosis? Bone 27, 1–3.

Ding, M., Day, J.S., Burr, D.B., Mashiba, T., Hirano, T., Weinans, H., Sumner, D.R., Hvid, I., 2003. Canine cancellous bone microarchitecture after one year of high-dose bisphosphonates. Calcified Tissue International 72 (6), 737–744.

Dufresne, T.E., Chmielewski, P.A., Manhart, M.D., Johnson, T.D., Borah, B., 2003. Risedronate preserves bone architecture in early postmenopausal women in 1 year as measured by three-dimensional microcomputed tomography. Calcified Tissue International 73 (5), 423–432.

Eriksen, E.F., Melsen, F., Sod, E., Barton, I., Chines, A., 2002. Effects of long-term risedronate on bone quality and bone turnover in women with postmenopausal osteoporosis. Bone 31, 620–625.

Forwood, M.R., Burr, D.B., Takano, Y., Eastman, D.F., Smith, P.N., Schwardt, J.D., 1995. Risedronate treatment does not increase microdamage in the canine femoral neck. Bone 16 (6), 643–650.

Frost, H.M., 1969. Tetracycline-based histological analysis of bone remodeling. Calcified Tissue International 3, 211–237.

Frost, H.M., 1998. Osteoporoses: a rationale for further definitions? Calcified Tissue International 62 (2), 89–94.

Hazelwood, S.J., Martin, R.B., Rashid, M.M., Rodrigo, J.J., 2001. A mechanistic model for internal bone remodeling exhibits different dynamic responses in disuse and overload. Journal of Biomechanics 34, 299–308.

Hirano, T., Turner, C.H., Forwood, M.R., Johnston, C.C., Burr, D.B., 2000. Does suppression of bone turnover impair mechanical properties by allowing microdamage accumulation? Bone 27 (1), 13–20.

Komatsubara, S., Mori, S., Mashiba, T., Ito, M., Li, J., Kaji, Y., Akiyama, T., Miyamoto, K., Cao, Y., Kawanishi, J., Norimatsu, H., 2003. Long-term treatment of incadronate disodium accumulates microdamage but improves the trabecular bone microarchitecture in dog vertebra. Journal of Bone and Mineral Research 18 (3), 512–520.

Komatsubara, S., Mori, S., Mashiba, T., Li, J., Nonaka, K., Kaji, Y., Akiyama, T., Miyamoto, K., Cao, Y., Kawanishi, J., Norimatsu, H., 2004. Suppressed bone turnover by long-term bisphosphonate treatment accumulates microdamage but maintains intrinsic material properties in cortical bone of dog rib. Journal of Bone and Mineral Research 19, 999–1005.

Martin, R.B., 1985. The usefulness of mathematical models for bone remodeling. Yearbook of Physical Anthropology 28, 227–236.

Martin, R.B., 1995. Mathematical model for repair of fatigue damage and stress fracture in osteonal bone. Journal of Orthopaedic Research 13, 309–316.

Mashiba, T., Hirano, T., Turner, C.H., Forwood, M.R., Johnston, C.C., Burr, D.B., 2000. Suppressed bone turnover by bisphosphonates increases microdamage accumulation and reduces some biomechanical properties in dog rib. Journal of Bone and Mineral Research 15 (4), 613–620.

Mashiba, T., Mori, S., Burr, D.B., Komatsubara, S., Cao, Y., Manabe, T., Norimatsu, H., 2005. The effects of suppressed bone remodeling by bisphosphonates on microdamage accumulation and degree of mineralization in the cortical bone of dog rib. Journal of Bone and Mineral Research 23 (Supplement), 36–42.

Mashiba, T., Turner, C.H., Hirano, T., Forwood, M.R., Johnston, C.C., Burr, D.B., 2001. Effects of suppressed bone turnover by bisphosphonates on microdamage accumulation and biomechanical properties in clinically relevant skeletal sites in beagles. Bone 28, 524–531.

Miller, P.D., Watts, N.B., Licata, A.A., Harris, S.T., Genant, H.K., Wasnich, R.D., Ross, P.D., Jackson, R.D., Hoseyni, M.S., Schoenfeld, S.L., Valent, D.J., Chesnut, C.H., 1997. Cyclical etidronate in the treatment of postmenopausal osteoporosis: efficacy and safety after seven years of treatment. American Journal of Medicine 103 (6), 468–476.

Moore, T.L.A., Gibson, L.J., 2002. Microdamage accumulation in bovine trabecular bone in uniaxial compression. Journal of Biomechanical Engineering—Transactions of the ASME 124 (1), 63–71.

Mori, S., Burr, D.B., 1993. Increased intracortical remodeling following fatigue damage. Bone 14, 103–109.

Nyman, J.S., Rodrigo, J.J., Hazelwood, S.J., Yeh, O.C., Martin, R.B., 2006. Predictions on preserving bone mass in knee arthroplasty with bisphosphonates. Journal of Arthroplasty 21 (1), 106–113.

Nyman, J.S., Yeh, O.C., Hazelwood, S.J., Martin, R.B., 2004. A theoretical analysis of long-term bisphosphonate effects on trabecular bone volume and microdamage. Bone 35, 296–305.

Porras, A.G., Holland, S.D., Gertz, B.J., 1999. Pharmacokinetics of alendronate. Clinical Pharmacokinetics 36, 315–328.

Recker, R.R., Gallagher, R., MacCosbe, P.E., 2005. Effect of dosing frequency on bisphosphonate medication adherence in a large longitudinal cohort of women. Mayo Clinic Proceedings 80 (7), 856–861.

Rodan, G.A., Fleisch, H.A., 1996. Bisphosphonates: mechanisms of action. Journal of Clinical Investigation 97 (12), 2692–2696.

Schaffler, M.B., Choi, K., Milgrom, C., 1995. Aging and matrix microdamage accumulation in human compact bone. Bone 17, 521–525.

Ste-Marie, L.G., Sod, E., Johnson, T., Chines, A., 2004. Five years of treatment with risedronate and its effects on bone safety in women with postmenopausal osteoporosis. Calcified Tissue International 75 (6), 469–476.

Storm, T., Steiniche, T., Thamsborg, G., Melsen, F., 1993. Changes in bone histomorphometry after long-term treatment with intermittent, cyclic etidronate for postmenopausal osteoporosis. Journal of Bone and Mineral Research 8, 199–208.

Tonino, R.P., Meunier, P.J., Emkey, R., Rodriguez-Portales, J.A., Menkes, C.J., Wasnich, R.D., Bone, H.G., Santora, A.C., Wu, M., Desai, R., Ross, P.D., 2000. Skeletal benefits of alendronate: 7-year treatment of postmenopausal osteoporotic women. Phase III osteoporosis treatment study group. Journal of Clinical Endocrinology and Metabolism 85 (9), 3109–3115.

Wang, X., Niebur, G.L., 2006. Microdamage propagation in trabecular bone due to changes in loading mode. Journal of Biomechanics 39, 781–790.

Whalen, R.T., Carter, D.R., Steele, C.R., 1988. Influence of physical activity on the regulation of bone density. Journal of Biomechanics 21 (10), 825–837.

Zoehrer, R., Roschger, P., Paschalis, E.P., Hofstaetter, J.G., Durchschlag, E., Fratzl, P., Phipps, R., Klaushofer, K., 2006. Effects of 3- and 5-year treatment with risedronate on bone mineralization density distribution in triple biopsies of the iliac crest in postmenopausal women. Journal of Bone and Mineral Research 21 (7), 1106–1112.